

Lectures on Random Matrices (Spring 2025)

Lecture 12: Random Growth Models

Leonid Petrov

Wednesday, April 2, 2025*

Contents

1	Recap	2
1.1	Dyson Brownian Motion with Determinantal Structure	2
1.2	The BBP Phase Transition	2
1.3	Remark: Corners process with outliers	3
1.4	Goal today	3
2	A window into universality: Airy line ensemble	4
3	KPZ universality class: Scaling and fluctuations	5
3.1	Universality of random growth	5
3.2	KPZ equation	5
3.3	First discoveries	6
3.4	Effect of initial conditions	6
3.5	Remark: Gaussian Free Field in KPZ universality	6
4	Polynuclear Growth and Last Passage Percolation	7
4.1	Definition and single-layer PNG	7
4.2	Multiline PNG	8
4.3	KPZ mechanisms in the PNG growth	9
4.4	Mapping PNG to last passage percolation	10
4.5	Multipath LPP and the multilayer PNG	10
4.6	Convergence to the Airy line ensemble	11
4.7	Space-time limit and the directed landscape	11
4.8	Convergence to the directed landscape	12
L	Problems (due 2025-04-29)	12
L.1	PNG ordering	12

*[Course webpage](#) • [Live simulations](#) • [TeX Source](#) • Updated at 06:38, Wednesday 2nd April, 2025

1 Recap

In our last lecture, we explored the asymptotics of Dyson Brownian Motion with an outlier. We specifically focused on the phase transition that occurs when a rank-1 perturbation is applied to a random matrix ensemble.

1.1 Dyson Brownian Motion with Determinantal Structure

We established that for $\beta = 2$, the eigenvalues of the time-evolved process form a determinantal point process. The transition probability from an initial configuration $\mathbf{a} = (a_1 \geq \dots \geq a_N)$ to a configuration $\mathbf{x} = (x_1 \geq \dots \geq x_N)$ at time t is given by:

$$P(\lambda(t) = \mathbf{x} \mid \lambda(0) = \mathbf{a}) = N! \left(\frac{1}{\sqrt{2\pi t}} \right)^N \prod_{1 \leq i < j \leq N} \frac{x_i - x_j}{a_i - a_j} \det \left[\exp \left(- \frac{(x_i - a_j)^2}{2t} \right) \right]_{i,j=1}^N$$

This determinantal structure enabled us to derive the correlation kernel:

$$K_t(x, y) = \frac{1}{(2\pi)^2 t} \int \int \exp \left(\frac{w^2 - 2yw}{2t} \right) \bigg/ \exp \left(\frac{z^2 - 2xz}{2t} \right) \prod_{i=1}^n \frac{w - a_i}{z - a_i} \frac{dw dz}{w - z} \quad (1.1)$$

where the contours of integration are specified to maintain analytical properties.

1.2 The BBP Phase Transition

The central focus was the Baik-Ben Arous-Péché (BBP) phase transition that occurs with finite-rank perturbations of GUE matrices. For the rank-1 case, we analyzed:

$$A + \sqrt{t}G, \quad \text{where } A = \text{diag}(a\sqrt{n}, 0, \dots, 0)$$

Through asymptotic analysis using steepest descent methods, we identified three distinct regimes:

1. **Airy regime** ($a < 1$): The largest eigenvalue follows the Tracy-Widom GUE distribution, just as in the unperturbed case. The spike is too weak to escape the bulk.
2. **Critical regime** ($a = 1$): A transitional behavior occurs when $a = 1 + An^{-1/3}$, leading to a deformed Airy kernel:

$$\tilde{K}_{\text{Airy}}(\xi, \eta) = \frac{1}{(2\pi i)^2} \iint \frac{\exp \left\{ \frac{W^3}{3} - \xi W - \frac{Z^3}{3} + \eta Z \right\}}{W - Z} \frac{W - A}{Z - A} dW dZ$$

3. **Gaussian regime** ($a > 1$): The largest eigenvalue separates from the bulk, becoming an "outlier" centered at $a + 1/a$. Its fluctuations follow a Gaussian distribution rather than the Tracy-Widom law.

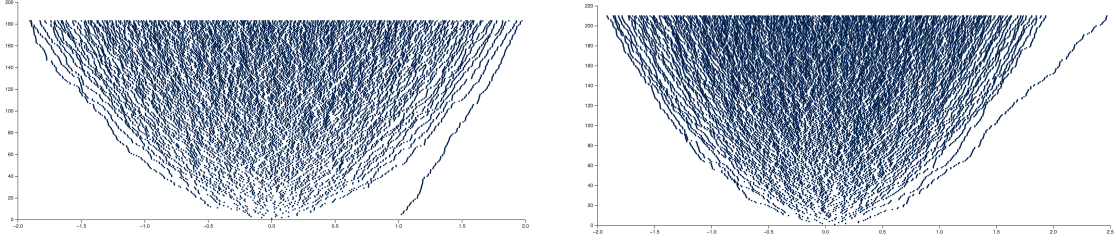


Figure 1: Two versions of the corners process with an outlier. Left: Corners process of $G + D$, where D is a rank-1 critical perturbation with eigenvalue 1. Right: Corners process of $G + UDU^\dagger$, where $U \in U(n)$ is a Haar-distributed unitary matrix and D is a rank-1 supercritical perturbation with eigenvalue 2 (the eigenvalue 1 is not visible in the rotated system). In both pictures, $n \approx 200$. See <https://lpetrov.cc/simulations/2025-03-27-orthogonal-corners-outliers/> for an interactive simulation.

1.3 Remark: Corners process with outliers

One can also perturb the corners process structure, and get correlation kernels similar to (1.1) which we had for the Dyson Brownian Motion. The perturbed corners process is considered in [FF14], see also the earlier work [Met13] for the corners process of UDU^\dagger , where D is arbitrary and U is Haar-distributed. Both the kernels for the Dyson Brownian Motion and the corners process with outliers can be obtained from the formula of [Met13]. See Figure 1 for an illustration of the corners process with an outlier in two cases, when the basis for the outlier is rotated or not (the rotation does not affect the top level eigenvalue distribution, but has a significant effect on the whole corners process).

1.4 Goal today

Today, the goal is to survey various objects which arise in the KPZ universality class:

- The Airy line ensemble, which is the universal edge scaling limit of Dyson Brownian Motion, the corners process, and numerous statistical physics models.
- Moreover, the Airy line ensemble arises and is fundamental for a class of random growth models in one space and one time dimensions, which is known as the KPZ universality class.
- We will briefly mention how the Gaussian Free Field (GFF) arises in the KPZ class models in two space dimensions.
- We continue to discuss one particular model in the KPZ universality class — the Polynuclear Growth (PNG) and the related Last Passage Percolation (LPP) models.

2 A window into universality: Airy line ensemble

The edge scaling limit of Dyson Brownian Motion and the corners process¹ is a universal object for $\beta = 2$ models and determinantal structures (and far beyond). GUE formulas provide us with a powerful lens through which to examine these universality phenomena. In this section, we discuss the limiting behavior of Dyson Brownian Motion near the spectral edge, highlighting two of its fundamental properties: Brownian Gibbs property and characterization.

Theorem 2.1 (Edge scaling limit to Airy line ensemble). *Consider an $N \times N$ GUE (Gaussian Unitary Ensemble) Dyson Brownian motion, i.e., the stochastic process of eigenvalues $(\lambda_1(t) \geq \dots \geq \lambda_N(t))_{t \in \mathbb{R}}$ evolving under Dyson's eigenvalue dynamics. After centering at the spectral edge parallel to the vector \mathbf{v}_t and applying the Airy scaling (tangent axis scaled by $N^{-1/3}$ and fluctuations scaled by $N^{-1/6}$), the top k eigenvalue trajectories converge as $N \rightarrow \infty$ to the **Airy line ensemble**. In particular, for each fixed $k \geq 1$ the rescaled process*

$$(N^{1/6}[\lambda_i(\langle N^{-1/3}, N^{-1/6} \rangle \cdot \mathbf{v}) - c_{N,t}])_{1 \leq i \leq k}$$

converges in distribution (uniformly on compact t -intervals) to $(\mathcal{P}_i(t))_{1 \leq i \leq k}$, where $\{\mathcal{P}_i(t)\}_{i \geq 1}$ is the parabolic Airy line ensemble.

Remark 2.2. The random variable $\mathcal{P}_1(0)$ has the GUE Tracy-Widom distribution.

Theorem 2.3 (Airy line ensemble is Brownian Gibbsian [CH16]). *The parabolic Airy line ensemble $\{\mathcal{P}_i(t)\}_{i \geq 1}$ satisfies the **Brownian Gibbs property**. Namely, for any fixed index $k \geq 1$ and any finite time interval $[a, b]$, conditioning on the outside portions of the ensemble (i.e., $\{\mathcal{P}_j(t) : t \notin [a, b]\}$ for all j , and $\{\mathcal{P}_j(t) : j \neq k\}$ for $t \in [a, b]$), the conditional law of the k th curve on $[a, b]$ is that of a **Brownian bridge** from $(a, \mathcal{P}_k(a))$ to $(b, \mathcal{P}_k(b))$ **conditioned** to stay above the $(k+1)$ th curve and below the $(k-1)$ th curve on $[a, b]$. In particular, the Airy line ensemble is invariant under this resampling of a single curve by a conditioned Brownian bridge.*

Theorem 2.4 (Characterization of ALE [AH23]). *The parabolic Airy line ensemble is the **unique** Brownian Gibbs line ensemble satisfying a natural parabolic curvature condition on the top curve. More precisely, let $\mathcal{P} = (\mathcal{P}_1, \mathcal{P}_2, \dots)$ be any line ensemble that satisfies the Brownian Gibbs property. Suppose in addition that the top line $\mathcal{P}_1(t)$ **approaches a parabola** of curvature $1/\sqrt{2}$ at infinity. Then \mathcal{L} must coincide (in law) with the **parabolic Airy line ensemble**, up to an overall affine shift of the entire ensemble.*

Let us define $\mathcal{L}_i(t) = \mathcal{P}_i(t) + t^2$, and call \mathcal{L} the Airy Line Ensemble (without the word “parabolic”). One can think that the parabola comes from the scaling window, which is of different proportions in the horizontal and vertical directions. The non-parabolic Airy line ensemble \mathcal{L} is time-stationary, that is, its distribution is invariant under time shifts $t \mapsto t + c$.

¹Both without outliers — the presence of critical outliers may add a few extra lines (wanderers) to the Airy line ensemble, and we will not consider this complication here.

3 KPZ universality class: Scaling and fluctuations

3.1 Universality of random growth

In the $(1+1)$ -dimensional **KPZ universality class**, random growth models exhibit a distinctive scale of fluctuations fundamentally different from classical Gaussian behavior. Kardar, Parisi, and Zhang [KPZ86] predicted that such interfaces have *roughness exponent* $1/2$ and *growth exponent* $1/3$, meaning that if time is scaled by a factor T , then horizontal distances scale by $T^{2/3}$ and vertical height fluctuations scale by $T^{1/3}$ [Rem22], as $T \rightarrow \infty$. Equivalently, the interface height $h(t, x)$ (after subtracting its deterministic mean growth) satisfies the $1 : 2 : 3$ *scaling*:

$$t^{-1/3} \left(h(t, \chi t^{2/3}) - \mathbb{E}[h(t, \chi t^{2/3})] \right) \quad \text{converges in law as } t \rightarrow \infty.$$

These exponents $2/3$ and $1/3$ are universal in one-dimensional growth with local randomness, distinguishing the KPZ class from, e.g., diffusive (Edwards–Wilkinson) interfaces. Intuitively, the interface develops random peaks of size $O(t^{1/3})$, and correlations spread over a spatial range $O(t^{2/3})$ —a highly nontrivial, super-diffusive scaling.

3.2 KPZ equation

The KPZ equation is a continuous model of random growth which was first proposed non-rigorously in the physics literature [KPZ86], and then justified mathematically. There are several justifications, including the one by Hairer [Hai14]. The equation reads (ignoring the constant by the terms in the right-hand side):

$$\partial_t h(t, x) = \partial_{xx} h(t, x) + (\partial_x h(t, x))^2 + \xi(t, x), \quad t > 0, \quad x \in \mathbb{R}, \quad (3.1)$$

where ξ is the space-time white noise, that is, a Gaussian process with

$$\mathbb{E}[\xi(t, x)\xi(t', x')] = \delta(t - t')\delta(x - x').$$

The terms in the KPZ equation stand for the three types of interactions driving the random growth process:

- The first term $\partial_{xx} h$ is a *smoothing* heat equation term, which is a classical diffusion (independent growth) term.
- The second term $(\partial_x h)^2$ is a *slope-dependent growth* term, which tends to close high-slope gaps. This mechanism is visible in discrete models which we will see in Section 4.
- The third term $\xi(t, x)$ is a *stochastic noise* term which favors independent growth at each location. This leads to roughening of the interface.

Note that the equation (3.1) is ill-posed even in the sense of distributions, since squaring a distribution $\partial_x h$ is not well-defined. Instead, to solve the KPZ equation in one space dimension $x \in \mathbb{R}$, one can formally write $h = \log Z$, where Z then solves the well-posed *stochastic heat equation* (SHE) with multiplicative noise:

$$\partial_t Z(t, x) = \partial_{xx} Z(t, x) + \xi(t, x)Z(t, x).$$

The stochastic heat equation is linear in Z , and there are no issues with defining the solution. The passage from h to $Z = \exp(h)$ is known as the *Cole-Hopf transformation*. It is not rigorous either, but was used prior to [Hai14] to define what it means to have a solution to (3.1).

3.3 First discoveries

One of the most striking discoveries is that the **one-point distribution** of these fluctuations, when the growth starts from the so-called *droplet* (or *narrow wedge*) initial condition, is governed by the GUE *Tracy–Widom law*, rather than a normal law. The **Tracy–Widom distribution** (for Gaussian Unitary Ensemble, GUE) describes the fluctuations of the largest eigenvalue of a random Hermitian matrix. In the KPZ class, the same distribution emerges in the long-time limit for a wide range of models and initial conditions. For example, in the Totally Asymmetric Simple Exclusion Process (TASEP) with step initial data (corresponding to the narrow wedge), the height at the origin, when centered and scaled by $t^{1/3}$, converges in law to the Tracy–Widom GUE distribution [Joh00], [Rem22]. This was the first rigorous confirmation of $1/3$ fluctuations in a random growth model. Such behavior is believed to be *universal*: many other integrable models (polynuclear growth, last-passage percolation, directed polymers, etc.) exhibit the same long-time distribution and scaling exponents.

In the next Section 4, we will discuss a particular semi-discrete random growth model — the Polynuclear Growth (PNG).

3.4 Effect of initial conditions

Crucially, the exact form of the Tracy–Widom limit depends on the *initial condition* of the growth process. Different symmetry classes of random matrices appear:

- **Curved (droplet) initial data:** Starting from a narrow peak (often called *narrow wedge* or *droplet* initial condition), the height fluctuations follow the Tracy–Widom GUE distribution in the $t \rightarrow \infty$ limit. This corresponds to the *unitary* symmetry class (e.g. complex Hermitian matrices).
- **Flat initial data:** Starting from a flat interface (e.g. all zero initial height), fluctuations converge to the Tracy–Widom GOE distribution, which is the law of the largest eigenvalue of a random real symmetric (Gaussian orthogonal ensemble) matrices, with *orthogonal* symmetry.
- **Stationary initial data:** Starting from a two-sided Brownian or otherwise stationary initial profile, the fluctuation distribution is again non-Gaussian but neither GOE nor GUE. In this case one obtains the *Baik–Rains distribution*, often denoted F_0 , which was first derived by Baik and Rains for a stationary last passage percolation model [BR00].

3.5 Remark: Gaussian Free Field in KPZ universality

The KPZ equation (3.1) can be posed in any space dimension:

$$\partial_t h(t, x) = Dh(t, x) + (\nabla h(t, x))^2 + \xi(t, x), \quad t > 0, \quad x \in \mathbb{R}^d,$$

where D is a second-order differential operator, and ∇ is the gradient. In $d = 2$ case, the operator D can have one of the two signatures:

$$D = \Delta \quad \text{or} \quad D = \partial_x^2 - \partial_y^2.$$

These two cases are known as *isotropic* and *anisotropic* KPZ equations, respectively.

The isotropic KPZ equation is much more mysterious than the anisotropic one. In the anisotropic case, it is believed that the fluctuations scale with exponent 0 (as opposed to $1/3$ for one dimension), while in the isotropic case, even the hypothetical fluctuation scaling exponent is debated.

Further evidence for the anisotropic case is the existence of exactly solvable growth models in this class (e.g., [BF14]), which have logarithmic fluctuations. Moreover, their fluctuations are governed by the Gaussian Free Field (GFF), which we encountered earlier in [Lecture 9](#). Moreover, the GFF should be the stationary distribution for the anisotropic KPZ fixed point (Markov process which should be the long-time scaling limit of the anisotropic KPZ equation).

Back to random matrices, consider the following question:

Can we imagine a 2-dimensional random growth model on random matrices, which will look like the 2-dimensional anisotropic KPZ equation? It would have random growth features, where some 2-dimensional surface is growing, and will have the GFF fluctuations.

We know an object in random matrices with GFF fluctuations — the height function of the corners process. So, a natural guess is to take the Brownian motion on matrix elements, and look at the evolution of the corners eigenvalues. However, the evolution of the eigenvalues of all corners is *not* going to be Markov. A workaround is the construction by Warren [War07], which produces the relevant Markov process on the full interlacing corners configuration.

4 Polynuclear Growth and Last Passage Percolation

4.1 Definition and single-layer PNG

We start with the *single-layer* PNG model on the real line. The interface height $h(t, x)$ evolves in continuous time $t \geq 0$ over the spatial coordinate $x \in \mathbb{R}$ and has piecewise-constant plateaus with sharp upward steps. In other words, $h(t, x)$ is piecewise constant in x , and takes integer values.

Dynamics. The evolution is described by two basic ingredients:

1. *Nucleation events:* At random times and locations (t, x) in the plane, a new “island” of height 1 is born atop the existing surface. Each newly born island sits just above $h(t, x)$, creating a step of height 1 at the precise point x and time t . We assume that the nucleation events form a Poisson process in space-time (t, x) .
2. *Lateral spread:* Once an island is created at height $k + 1$, its boundaries spread outward (to the left and right in x) with speed 1. Thus a step boundary moves in both directions until it merges with another step boundary or nucleation event. When the islands merge, the height becomes flat at this point.

See Figure 2 for an illustration of the single-layer PNG model. See also Figure 3 for an evolution of the nucleation events, each of which spreads at speed 1.

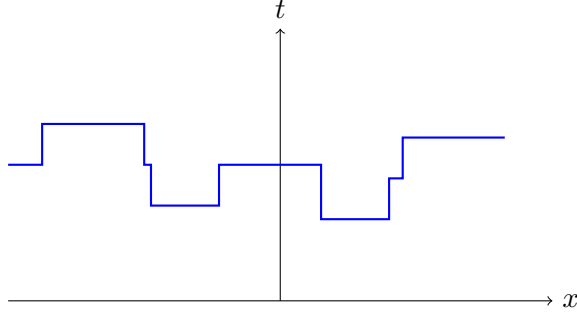


Figure 2: Polynuclear Growth (PNG) model interface.

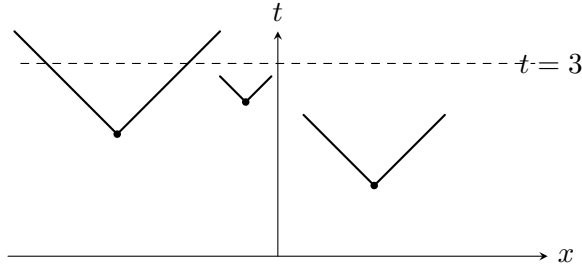


Figure 3: Single-layer PNG: Nucleations (black dots) appear randomly in the (t, x) plane according to a Poisson process. Each nucleation creates an upward step of height 1. The boundary of each newly created island expands laterally at speed 1.

Initialization. One typically imposes an initial condition $h(0, x)$ on the spatial axis (e.g., a single spike or droplet, or a flat interface). The flat interface is $h(0, x) = 0$ for all $x \in \mathbb{R}$, and the droplet is a single upward step at $x = 0$ with height 1. In the droplet case, we also set $h(0, x) = -\infty$ for $x \neq 0$, for convenience.

4.2 Multiline PNG

The *multiline* version of PNG tracks multiple height levels by stacking interfaces at multiple layers, $h_k(t, x)$. A merging event at layer k produces a nucleation event at layer $k + 1$. So, the nucleation at h_1 is powered by the Poisson process, while the nucleation at each h_k , $k \geq 2$, is powered by the merges at h_{k-1} . The initial condition is assumed to satisfy

$$h_1(0, x) \geq h_2(0, x) \geq \cdots, \quad \text{for all } x \in \mathbb{R}.$$

This ordering is preserved by the evolution, see Problem L.1.

We see that the evolution of h_2, h_3, \dots is just a function of the full space-time evolution of h_1 . However, at fixed time t , the functions $h_k(t, \cdot)$ cannot be determined just by $h_1(t, \cdot)$.

4.3 KPZ mechanisms in the PNG growth

Let us compare the single-layer PNG growth with the ingredients of the KPZ equation [\(3.1\)](#):

-

4.4 Mapping PNG to last passage percolation

One of the most important viewpoints is that a single-layer PNG interface can be encoded by a *directed last passage percolation* (LPP) model in a *Poisson* random environment. Concretely, suppose that nucleations occur according to a homogeneous Poisson point process of intensity 1 in the upper half-plane $\{(t, x) : t > 0, x \in \mathbb{R}\}$. Then each point (t, x) is the birth of an island at height 1 above the existing interface.

Steps as up-right paths. Define a time-axis t (vertical) and space-axis x (horizontal). If we track one upward step boundary from the moment of nucleation at (t, x) , it extends leftward with speed 1 (slope -1) and rightward with speed 1 (slope $+1$). For the boundary to persist until some later time $T > t$, it must not collide with any other step boundary that is seeded at a point (t', x') with $t' < T$.

LPP interpretation. For an up-right path π in the plane, let π pass only through space-time points with slope 1 or vertical steps. Then the “weight” of π can be defined as the number of Poisson points (nucleations) it encounters along the way. In last passage percolation, we seek a path that collects as many Poisson points as possible between given initial and final locations in the (t, x) plane. The maximal weight over all up-right paths is the *last passage time*. Figure 4 shows how Poisson points might lie in the plane, and how an up-right path might pass through them.

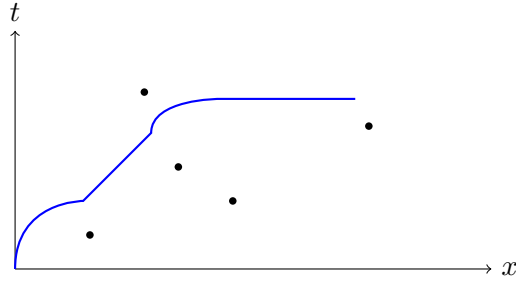


Figure 4: A Poisson scattering of nucleation points in the upper half-plane. An up-right path (blue) collects those points it passes through. The maximum number of points collected by a path from $(t, x) = (0, 0)$ to (T, X) encodes the PNG height above X at time T .

Equivalence of height and last passage time. In a classical result (sometimes called the Robinson–Schensted correspondence in continuous form), one finds that the PNG height at a given location/time is exactly the maximal number of Poisson points an up-right path can collect on its way to that location/time. This equivalence extends to *multipath* last passage percolation, mirroring how multiline PNG arises from multiple nested up-right paths that do not intersect.

4.5 Multipath LPP and the multilayer PNG

We now see how the *multi-layer* PNG from Subsection 4.2 matches a *multipath* version of LPP. Suppose we fix M layers in the PNG, or equivalently fix M nonintersecting up-right paths in the Poisson environment. Each path tries to collect as many Poisson points as possible, subject to

the constraint that the paths remain strictly nonintersecting (e.g., we can number them from top to bottom).

- The bottom path corresponds to the first layer $h_1(t, x)$. It accumulates a maximal number of Poisson points among all up-right paths from, say, $(0, -\infty)$ to (t, x) .
- The second path is forced to stay above the first path and thus sees fewer available points. This path corresponds to the second PNG layer $h_2(t, x)$, etc.

We have thus a bijection between these nonintersecting LPP paths and multiline PNG interfaces. Such a direct connection is a key source of *integrable structure*: the nonintersecting property implies determinantal formulas for correlation functions, reminiscent of the GUE corner processes or noncolliding random walks.

4.6 Convergence to the Airy line ensemble

A celebrated result is that *one-dimensional PNG* with droplet (narrow wedge) initial condition has a natural large-time scaling limit in which the top interfaces (equivalently, the highest LPP paths) converge in distribution to the Airy line ensemble. Precisely, one considers the interface height $h(t, x)$ around its deterministic shape function (the “hydrodynamic limit”) and rescales time, space, and fluctuations by the $t^{2/3}/t^{1/3}$ exponents of the KPZ class. More explicitly:

- Let t be large, and recenter the interface $h(t, x)$ about its mean shape $H_{\text{det}}(t, x)$ (which is on the order of t).
- Rescale x by $t^{2/3}$ and h by $t^{1/3}$.
- Track the top several layers as $i = 1, 2, \dots$.

Under these scalings, the joint distribution of $(h_i(t, x) - H_{\text{det}}(t, x))_{i \geq 1}$ converges as $t \rightarrow \infty$ to the parabolic Airy line ensemble. Consequently, the top layer’s fluctuations at a single spatial point converge to the GUE Tracy–Widom distribution, matching the predictions of the KPZ universality class.

4.7 Space-time limit and the directed landscape

While the convergence to the Airy line ensemble describes *fixed* time t (or equivalently a single horizontal slice in last passage percolation), one can pose the deeper question: can we capture the full *two-dimensional* limiting field $h(t, x)$ in space and time simultaneously?

Specifically, define

$$H_t^{\text{PNG}}(x) = h(t, x\sqrt{2}) - (\text{deterministic parabola}),$$

then rescale t, x in the KPZ 1 : 2 : 3 fashion. One expects that

$$\left(H_t^{\text{PNG}}(x) \right)_{x \in \mathbb{R}, t \geq 0} \implies \left(\mathcal{H}(T, X) \right)_{X \in \mathbb{R}, T \geq 0},$$

where $\mathcal{H}(T, X)$ is a random field capturing the universal space-time geometry of KPZ fluctuations. We desire a description of \mathcal{H} by some universal stochastic partial differential equation or otherwise.

4.8 Convergence to the directed landscape

The limiting object conjectured (and now proven in many integrable models) is the *directed landscape*, a continuous random function of $(t_1, x_1; t_2, x_2)$ with $t_2 > t_1$, representing the *limiting last passage percolation* metric in the plane. Concretely:

- The directed landscape \mathcal{L} assigns a “length” $\mathcal{L}(t_1, x_1; t_2, x_2)$ to every up-right path from (t_1, x_1) to (t_2, x_2) .
- This \mathcal{L} is the universal scaling limit of planar LPP and PNG with Poisson or geometric weights, capturing the entire space-time evolution (not just single-time slices).
- Restricting to a single time t_2 with initial time $t_1 = 0$, one recovers the top layer fluctuations converging to the Airy line ensemble. Thus the directed landscape is an enrichment that glues all times together consistently.

For the PNG model started from a droplet initial condition, the interface height converges under the 1 : 2 : 3 scaling to $\max_{x_1} \{\mathcal{L}(0, x_1; t, x)\}$, providing a universal limit shape and fluctuation field.

Thus the polynuclear growth viewpoint not only reproduces the core Tracy–Widom and Airy line ensemble phenomena (from single-time slices) but also paves the way to the more refined *directed landscape*, which describes all space-time evolution in a single universal object.

L Problems (due 2025-04-29)

L.1 PNG ordering

If the initial conditions at time 0 of the multiline PNG satisfy

$$h_1(0, x) \geq h_2(0, x) \geq \cdots, \quad \text{for all } x \in \mathbb{R},$$

then show that they continue to satisfy the same ordering at all times $t > 0$.

References

- [AH23] A. Aggarwal and J. Huang, *Strong Characterization for the Airy Line Ensemble*, arXiv preprint (2023). arXiv:2308.11908. [↑4](#)
- [BF14] A. Borodin and P. Ferrari, *Anisotropic growth of random surfaces in 2+1 dimensions*, Commun. Math. Phys. **325** (2014), 603–684. arXiv:0804.3035 [math-ph]. [↑7](#)
- [BR00] J. Baik and E. Rains, *Limiting distributions for a polynuclear growth model with external sources*, Jour. Stat. Phys. **100** (2000), no. 3, 523–541. arXiv:math/0003130 [math.PR]. [↑6](#)
- [CH16] I. Corwin and A. Hammond, *KPZ line ensemble*, Probability Theory and Related Fields **166** (2016), no. 1-2, 67–185. arXiv:1312.2600 [math.PR]. [↑4](#)
- [FF14] P. Ferrari and R. Frings, *Perturbed GUE minor process and Warren’s process with drifts*, J. Stat. Phys. **154** (2014), no. 1-2, 356–377. arXiv:1212.5534 [math-ph]. [↑3](#)
- [Hai14] M. Hairer, *Solving the KPZ equation*, Ann. Math. (2) **178** (2014), no. 2, 559–664. arXiv:1109.6811 [math.PR]. [↑5](#), [6](#)

- [Joh00] K. Johansson, *Shape fluctuations and random matrices*, Commun. Math. Phys. **209** (2000), no. 2, 437–476. arXiv:math/9903134 [math.CO]. [↑6](#)
- [KPZ86] M. Kardar, G. Parisi, and Y. Zhang, *Dynamic scaling of growing interfaces*, Physical Review Letters **56** (1986), no. 9, 889. [↑5](#)
- [Met13] A. Metcalfe, *Universality properties of Gelfand-Tsetlin patterns*, Probab. Theory Relat. Fields **155** (2013), no. 1-2, 303–346. arXiv:1105.1272 [math.PR]. [↑3](#)
- [Rem22] D. Remenik, *Integrable fluctuations in the KPZ universality class*, Proc. Int. Congr. Math. 2022 (2022), 4426–4450. arXiv:2205.01433 [math.PR]. [↑5](#), [6](#)
- [War07] J. Warren, *Dyson’s Brownian motions, intertwining and interlacing*, Electron. J. Probab. **12** (2007), no. 19, 573–590. arXiv:math/0509720 [math.PR]. [↑7](#)

L. PETROV, UNIVERSITY OF VIRGINIA, DEPARTMENT OF MATHEMATICS, 141 CABELL DRIVE, KERCHOF HALL, P.O. BOX 400137, CHARLOTTESVILLE, VA 22904, USA
 E-mail: lenia.petrov@gmail.com